ELSEVIER

Contents lists available at ScienceDirect

Results in Materials

journal homepage: www.sciencedirect.com/journal/results-in-materials





Phase formation, microstructural and superconducting properties of YBCO added Ca-compounds extraction eggshells

Siew Hong Yap ^a, Mohd Mustafa Awang Kechik ^{a,*}, Syahrul Humaidi ^{b,**}, Khairul Khaizi Mohd Shariff ^c, Hussien Baqiah ^d, Soo Kien Chen ^a, Kean Pah Lim ^a, Mohd Hafiz Mohd Zaid ^a, Yazid Yaakob ^a, Mohd Khalis Abdul Karim ^a, Zainal Abidin Talib ^e, Zhi Wei Loh ^a, Aliah Nursyahirah Kamarudin ^a, Abdul Halim Shaari ^a, Muralidhar Miryala ^f

- a Superconductor & Thin Films Laboratory, Department of Physics, Faculty of Science, Universiti Putra Malaysia, UPM Serdang, 43400, Selangor Darul Ehsan, Malaysia
- ^b Postgraduate Program (Physics), FMIPA, Universitas Sumatera Utara, Medan, 20222 Indonesia
- ^c Microwaye Research Institute, Universiti Teknologi MARA, 40450, Shah Alam, Selangor, Malaysia
- d Shandong Key Laboratory of Biophysics, Institute of Biophysics, Dezhou University, No. 566 University Rd. West, Dezhou, Shandong, China
- ^e Department of Physics, College of Natural Sciences, Jeonbuk National University, 567, Baekjedaero, Deokjingu, Jeonjusi, 54896, Jeollabukdo, Republic of Korea
- f Materials for Energy and Environmental Laboratory, Superconducting Materials Group, Graduate School of Science & Engineering, Shibaura Institute of Technology, 3-7-5 Foxesu, Koto-ku, Tokyo, 135-8548, Japan

ARTICLE INFO

Keywords: Critical temperature Ca-compounds Superconducting transition width Hole concentration Grains degradations

ABSTRACT

For several decades now, the emergence and production of high-quality bulk rare-earth-based superconductors, particularly YBa₂Cu₃O₇₋₈ (YBCO/Y-123), have been noteworthy advancements with potential implications in various fields. This unique research investigated the potential of using chicken eggshells as a source of calcium compounds (CaO, CaCO3 and Ca(OH)2) for the synthesis of YBCO. The green approach synthesis of YBCO added with Ca-compounds (0.0100 wt% $\leq x \leq$ 0.6000 wt%) was conducted in a systematic manner via thermal treatment method. The crystal structure, surface morphology, and chemical composition of the specimens were characterized by X-ray diffraction (XRD), Field Emission Scanning Electron Microscope (FESEM), and Energy Dispersive X-Ray Spectroscopy (EDX). The results showed the formation of orthorhombic Y-123 phase, Pmmm space group with the high-intensity peaks of Y-123. The addition of Ca-compounds proposed a different trend of grain degradations in the YBCO matrix system with the appearance of Ca-compounds' impurity phases. The superconducting properties such as electrical resistivity analyzed using electrical resistance measurement. Surprisingly, the superconducting parameters improved after Ca-compounds were added into the YBCO system. The hole concentration, p reached the highest value among all the specimens with the lowest superconducting transition width, $\sim \Delta T_{\rm c} = 3.805$ K ($T_{\rm c-onset} = 93.223$ K and $T_{\rm c(R=0)} = 89.418$ K) for the lowest concentration of Ca-compounds i.e., 0.0375 wt%. This great finding targeted the green approach impurity materials into YBCO system that can usefully enhance the superconducting properties at high temperature which covers the idea of addition with deficient concentration Ca-compounds.

1. Introduction

The discovery of bulk rare earth-based superconductors (REBa₂. Cu_3O_y /REBCO) greatly contributed to the development of the world in many aspects such as transportation [1–3], medical and technology [4–7]. It has emerged as a significant superconductor material achieved at high-field applications such as superconducting bearings, flywheel

energy storage systems, and bulk superconducting magnets. Fabrication of high-quality bulk rare earth-based superconductors is a longstanding research target since year 1990's. Among the various type of High Temperature Superconductors (HTS), $YBa_2Cu_3O_{7-\delta}$ (YBCO/Y-123) is the most practical and potential superconductor material for a wide range of technological applications among the copper-oxide family. Numerous methods were employed to synthesis a good quality superconductor

E-mail addresses: mmak@upm.edu.my (M.M. Awang Kechik), syahrul1@usu.ac.id (S. Humaidi).

https://doi.org/10.1016/j.rinma.2025.100661

^{*} Corresponding author.

^{**} Corresponding author.

from the copper-oxide family [8–16]. As known, the weak link behavior is caused by structural inhomogeneities, pores, voids limit, and impurity phases at grain boundaries of Y-123. Numerous efforts have been made to massively boost the superconducting transition width (ΔT_c) or critical current density (J_c) using the incorporations of artificial pinning centres (APCs) into the copper oxide system [4,17] such as addition of different type of metallic [18,19] and non-metallic elements, the inclusion of carbon-based compounds [20-24], swift heavy ion irration [25,26] and alkali metals [27-29]. Introduction of moderate amount of alkali earth metal is expected to improve grain boundary quality and grain connectivity of YBCO and at a certain amount may participate into fine particles that may act as APCs in the superconductors. To attain the better critical parameters, various methods of introducing APCs into the HTS in a manner regulated by its dimensions were employed [4,10,11, 20,21,30-33] with the aim to obtain materials with optimum oxygen content and main-phase structure. These methods included traditional solid-state reaction, co-precipitation, sol gel and melt processing. These methods were modified to improve superconducting properties.

At one point, alkali earth metal oxides are drawing substantial attention from a wide range of investigators in several sectors to create new and efficient ways to regulate and manufacture metal oxide nanostructures [34-37]. Thus, CaO reported as an important fundamental material in high- T_c superconductors [38,39] since previous technological applications. However, the metal oxide catalyst, CaO is quite costly than metal hydroxides such as Ca(OH)2 and NaOH. In terms of catalyst efficiency and economics, it is essential to obtain base heterogeneous catalysts extracted from natural materials at a low cost. Hence, we are sparking at a very economic and environmentally friendly household waste that is chicken eggshells. Chicken eggshells had been found containing calcium carbonate, CaCO₃ (94 %), calcium phosphate (1 %), organic compounds (4 %), and magnesium carbonate (1 %) [40]. The high contains of calcium in eggshells can be converted as a CaO catalyst by calcinations process at temperature around 900 °C for 2 h [41] where the reaction takes place as exothermic reaction. CaCO3, the major ingredient of eggshells, is known to decompose at temperature of 900 °C [41].

This study aims to investigate the superconducting and nonsuperconducting phases during the superconducting transitions within the YBCO system. We specifically investigate the effects of adding alkaline earth metals extracted from household waste, with a particular focus on Ca-compounds (CaO, CaCO3, and Ca(OH)2), highlighting the novelty of this approach. An eco-friendly synthesis and thermal treatment method was employed, known for its simplicity, cost-effectiveness, and ability to produce fine powders. By using aqueous solutions of metal nitrates and a polymer such as polyvinyl pyrrolidone (PVP) as a capping agent [13,14,29,42-44], this approach has many advantages. This thermal treatment method is considered environmentally friendly because it does not produce toxic gases during the process. Additionally, heat treatment is conducted over a short period, significantly saving electricity and making it suitable for large-scale applications. Therefore, extensive research is being conducted into the green synthesis of YBCO added with Ca-compounds in a systematic manner.

2. Materials and method

2.1. Specimen preparation

For the specimen preparation, stoichiometric amounts of high purity metal nitrates (\approx 99 %), i.e. Y(NO₃)₂·6H₂O, Ba(NO₃)₂, and Cu (NO₃)₂·2.5H₂O (Alfa Aesar) as starting materials mix with PVP. The solution was magnetically stirred and dried at 110 °C for 24 h. After the drying process, the green dry gel was crushed into fine powder. The green fine powder was pre-calcined at 600 °C for 4 h and calcined at 910 °C for 24 h in air after intermediate ground. The powdered form of specimens was reground after added with corresponding amount concentration of Ca-compounds extracted from chicken eggshells (CaES)

which been calcined at 900 $^{\circ}$ C for 2 h [41,45]. The grounded fine powders were then compressed into the circular pellets (about 15 mm thick and 13 mm diameter) using a hydraulic press with same pressure load. The pelletized specimens were sintered at a temperature of 980 $^{\circ}$ C for 24 h under ambient conditions.

2.2. Specimen investigation

The phase development and crystal structure of the specimens were studied using the X-ray diffraction (XRD) method on a PW 3040/60 MPD X'Pert Pro Panalytical Philips DY 1861 X-ray diffractometer with a Cu-K radiation source with the wavelength of 1.45 Å. The scanning was carried out in the 2θ range of $20^\circ-80^\circ$ with an increment step size of $0.03^\circ.$ The microstructure was studied by the FESEM and EDX using a model NOVA NANOSEM 230 instrument equipment with EDX. The superconducting properties i.e., electrical resistivity measurement of the specimens was measured using the inhouse homemade setup four-point probe technique.

3. Results and discussion

3.1. Structural and phase formation analysis

Fig. 1 shows the XRD patterns of the various concentration of CaES addition into YBCO with major phase YBa2Cu3O7-8 (Y-123) and other phases such as YBa₂Cu₃O₅ (Y-211) and BaCuO₂. The XRD characterization for Ca-compounds extraction from chicken eggshells (CaES) was done concurrently with all the specimens to proof the addition containing all Ca-compounds as shown in Fig. 2 This result explore that the CaES specimen were containing 44.4 % volume fraction of CaO (ICSD: 98-003-4917), 53.5 % volume fraction of Ca(OH)₂ (ICSD: 98-004-8798) and 2.1 % volume fraction of CaCO3 (ICSD: 98-002-1923). All the final specimens were verified with the formation of orthorhombic Y-123 phase, Pmmm space group (ICSD: 98-006-0398) with the high intensity peaks of Y-123 and it's found at $2\theta \approx 32.5^{\circ}$ and $2\theta \approx 32.8^{\circ}$. It agrees with Miller indices of (013) and (103), respectively. The orthorhombic crystal structure with the peaks for other phases such as Y-211 (ICSD: 98-002-9780) and $BaCuO_2$ (ICSD: 98-002-5029). This finding agrees with the previous works [9,42,46,47]. In-depth observations of the phases that developed in the specimens are provided in Table 1. With higher concentration of CaES addition such as 0.60000 wt% and 0.3000 wt%, there are some additional of other phases such as 0.4 % CaCuO2 (ICSD: 98-003-9756) at 0.3000 wt% and 1.4 % $Ba_4CaCu_3O_{8.61}$ (ICSD:

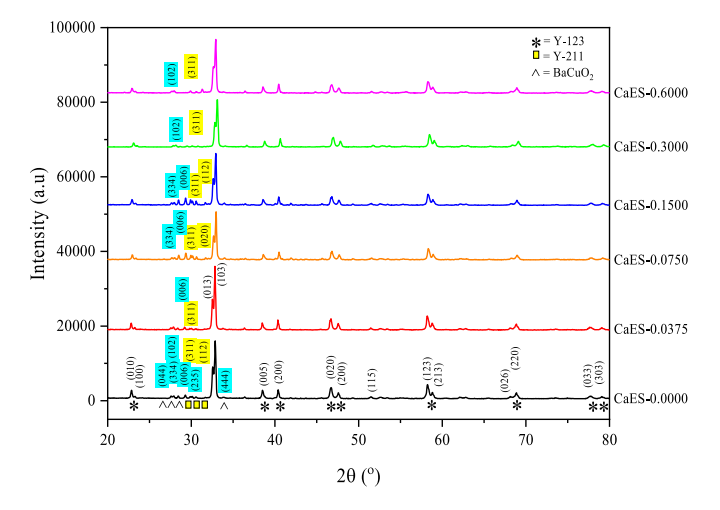


Fig. 1. XRD pattern for YBCO added with various concentration of CaES 0.0000 wt% (CaES-0.0000), 0.0375 wt% (CaES-0.0375), 0.0750 wt% (CaES-0.0750), 0.1500 wt% (CaES-0.1500), 0.3000 wt% (CaES-0.3000) and 0.6000 wt% (CaES-0.6000) sintered under ambient conditions.

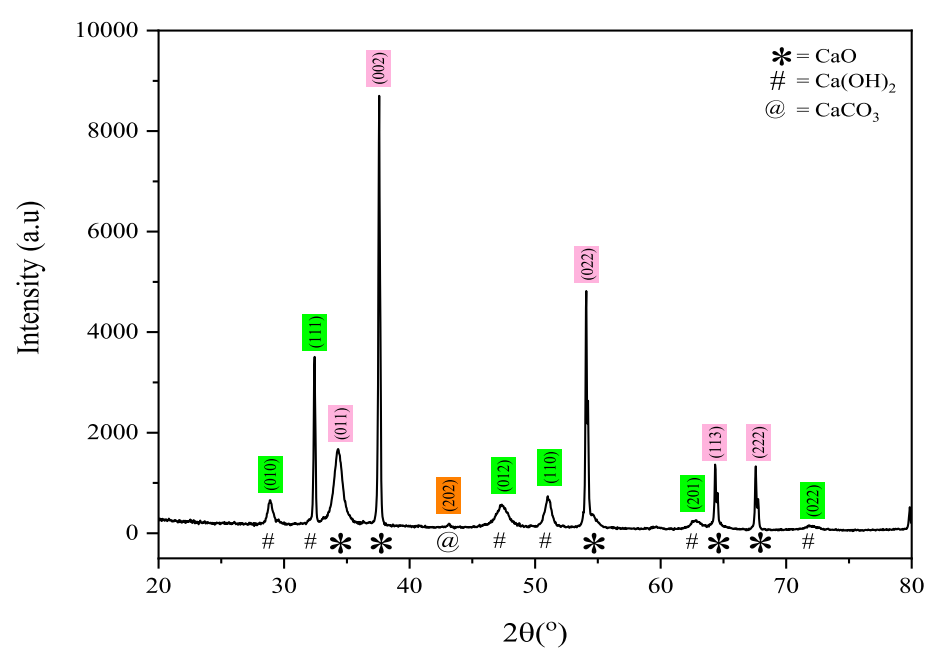


Fig. 2. XRD pattern of CaES calcined at 900 °C for 2 h.

Table 1
The volume fractions, unit cell volume of Y-123, FWHM, crystallite size, and lattice strain of YBCO added with various concentration of CaES sintered under ambient conditions.

Specimen	Volume Fract	ion				V ^a (Åm ³)	FWHM Y-123	CS ^b (Åm)	LS ^c (%)
	Y-123 (%)	Y-211 (%)	BaCuO ₂ (%)	CaCuO ₂ (%)	Ba ₄ CaCu ₃ O _{8.61} (%)				
CaES 0.0000	89.2	3.0	7.8	_	_	173.5520	0.1804	635	0.256
CaES 0.0375	94.4	3.6	1.9	_	_	173.2066	0.1604	673	0.224
CaES 0.0750	75.5	8.6	15.9	_	_	173.4983	0.1638	728	0.231
CaES 0.1500	75.2	9.8	15.0	_	_	173.4727	0.1709	685	0.242
CaES 0.3000	95.3	2.6	1.7	0.4	_	173.6890	0.1743	668	0.246
CaES 0.6000	93.4	4.9	0.3	_	1.4	173.6240	0.1784	645	0.253

^a V is Volume of Unit Cell Y-123.

98-002-7725) at 0.6000 wt%. This indicates with the addition of higher concentration more than 0.30 wt% and above, the CaES compounds such as CaO, $Ca(OH)_2$ and $CaCO_3$ reacted with Y-123 host matrix and resulted the formation of other Ca based compounds [48]. This mean that deficient concentration Ca in the YBCO system may generates unit cell defects but still maintain a good YBCO matrix system [49].

The lattice parameters (a,b) and (c) were determined through Rietveld refinement using the HighScore Plus software. Table 2 shows the variation of lattice parameters of the (a,b), and (c) axes, oxygen content, as well as Table 1 shows the unit cell volume, volume fractions, crystallites size and lattice strains of Y-123 computed from the XRD data of the specimens. From Table 2, the lattice parameters clearly show that all the specimens have an orthorhombic crystal structure. The lattice

parameters for Y-123 were in slight change and various trend after CaES addition into YBCO system as compared to pure YBCO. The obtained results furthering supported that Ca-compounds did not substitute into the Y-123 matrix system [50] but it entered into the inter-grain regions. The orthorhombicity value was posted as the highest values at the lowest concentration of CaES, 0.0375 wt%. The trend of orthorhombicity via concentration increased with the increasing of volume fraction of other phases such as Y-211 and BaCuO₂. The oxygen content in the Y-123 matrix for all addition specimens are approximately closed to 6.8 and in good agreement as reported before [51,52]. The value of the oxygen content was estimated by equation (7 – δ = 75.25–5.86 c), where c is lattice parameter on y-axis in YBCO matrix system [48,52]. We observed the lowest concentration of CaES had the highest value of

Table 2

The lattice parameters, orthorhombicity, and oxygen content for Y-123 with various concentration of CaES additions sintered under ambient conditions.

Specimen with wt.%	Lattice Parameter	s (Å)		Orthorhombicity	δ	$O_{7-\delta}$
	a-axis	b-axis	c-axis	(b-a)/(a+b)		
CaES 0.0000	3.8220(2)	3.8849(3)	11.6886(9)	0.00816	0.2452	6.7548
CaES 0.0375	3.8192(2)	3.8833(2)	11.6788(7)	0.00832	0.1878	6.8122
CaES 0.0750	3.8219(2)	3.8844(2)	11.6861(7)	0.00811	0.2305	6.7695
CaES 0.1500	3.8219(2)	3.8833(2)	11.6778(7)	0.00796	0.1819	6.8181
CaES 0.3000	3.8236(2)	3.8853(2)	11.6916(9)	0.00800	0.2628	6.7372
CaES 0.6000	3.8248(2)	3.8834(2)	11.6892(9)	0.00760	0.2487	6.7513

^b Cs is Crystallite Size Y-123.

c LS is Lattice Strain Y-123.

S.H. Yap et al. Results in Materials 26 (2025) 100661

orthorhombicity, showing that thinning twin borders is associated with increases in ordering oxygen throughout *b*-axis in Cu-O-Cu chain and an increase in twin density. Hence, we believe that the created thin twin boundaries which a good pining defects and can act as effective APCs that support good superconductivity properties [18].

From Table 1, we can observe that concentration CaES 0.0375 wt% has the lowest lattice strain, 0.224 %. It also reveals that the crystallite size of Y-123 for addition CaES 0.0375 wt%, 0.0750 wt% and 0.0150 wt % posted higher crystallite size as compare the higher concentration such as 0.3000 wt% and 0.6000 wt% specimens. This difference was most likely due to the lowest concentration of CaES causing more grain growth in the suitable ratio of other phases to occur such as Y-211 and BaCuO₂ at the grain boundary (Fig. 1 and Table 1). We proposed that the CaES added into YBCO system in the lowest concentration produced the right amount of other phases, Y-211 and BaCuO₂, at grain boundaries, which ensured the stability of the major phase composition, Y-123. As in Table 1, we found that at triple high concentration of CaES, 0.3000 wt% and 0.6000 wt% have created other impurity phases such as CaCuO2 and Ba₄CaCu₃O_{8.61} which we believed it caused the oxygen deficiency and increased the lattice strain of Y-123 with higher full width at half maximum (FWHM) in the YBCO matrix system. The lowest FWHM with the narrowest width of peak is ascribed to the uniform lattice strain that comes from the perfection of crystalline nature of the YBCO system [53].

3.2. Microstructural and elementals analysis

The surface morphologies and microstructure properties for all specimens were studied using the characteristic of FESEM as shown in Fig. 3. The average grain size was measured using the Image-J software from 100 grains picked at random and measured in both dimensions of the elongated grains as illustrated in Fig. 4. Subsequently, Figs. 3 and 5 show the FESEM images and grain sizes distribution histograms of all specimens respectively. All these specimens shown irregular shape and randomly distributed grains with size varied from 1 to 2 μm . Pores or voids defect were observed on the surface morphology. All average grain

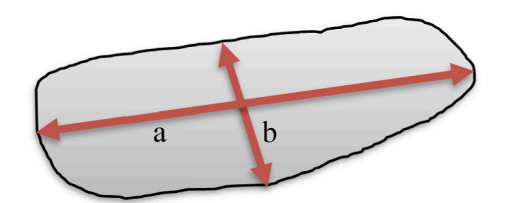


Fig. 4. A schematic diagram for measuring the average grain size of a selected single grain.

sizes for all specimens are shown in Table 3, in the lowest concentration of CaES, 0.0375 wt%, it posted a lower average grain size, ~1.4403 (± 0.5967) μm as compared to pure YBCO specimen, ~1.9887 (± 1.2873) µm. The surface morphology picture shows an alteration in grain refinement, which begins with the degradation of some larger grains into smaller grains after the addition of CaES. Also referred to the analysis of the grain size distribution histogram in Fig. 5, the grain distribution for 0.0375 wt% CaES shows the best homogenous distribution curve. Thus, with very low concentration of CaES addition might create a better grain alignment with less pores which will enhance superconductivity i.e., J_c [8] as compared to the higher concentration, such as 0.3000 wt% and above. With added a triple high concentration from 0.0375 wt% to 0.3000 wt%, there was another grains degradation and grains refinement happen on the surface morphology with the highest average grain size among all specimens that is ~1.5334 (± 0.7133) µm. After the concentration of 0.3000 wt%, with a double up amount of concentration, 0.6000 wt%, the average grain size was decreased again into $\sim 1.1794~(\pm 0.4912)~\mu m$. This means that the addition of CaES proposed a different trend of grains degradations and grains refinement in the YBCO matrix system with the appearance of Cacompounds impurity phases.

Fig. 6 shows the Energy-Dispersive X-ray (EDX) spectra of all specimens. It's confirmed that all specimens constituted of Y, Ba, Cu and O.

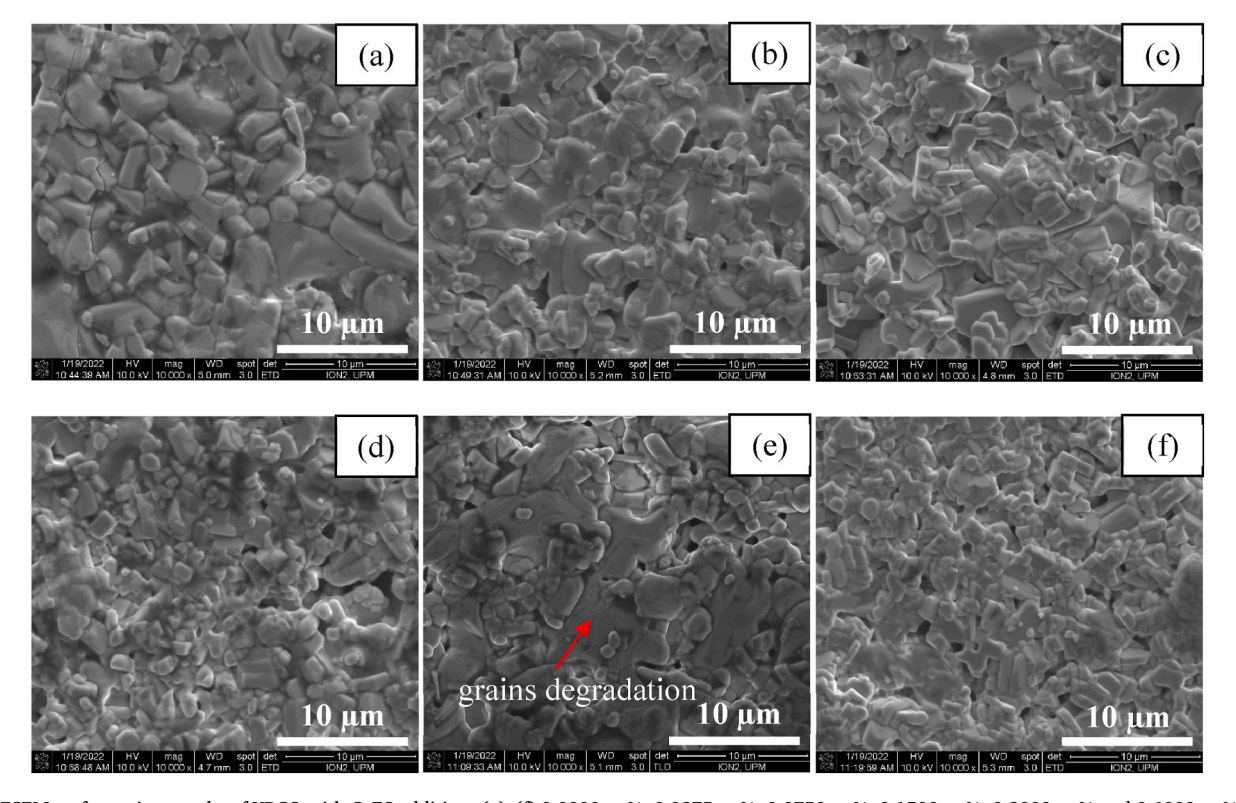


Fig. 3. FESEM surface micrographs of YBCO with CaES additions (a)—(f) 0.0000 wt%, 0.0375 wt%, 0.0750 wt%, 0.1500 wt%, 0.3000 wt% and 0.6000 wt% sintered under ambient conditions at 10,000x magnification, respectively.

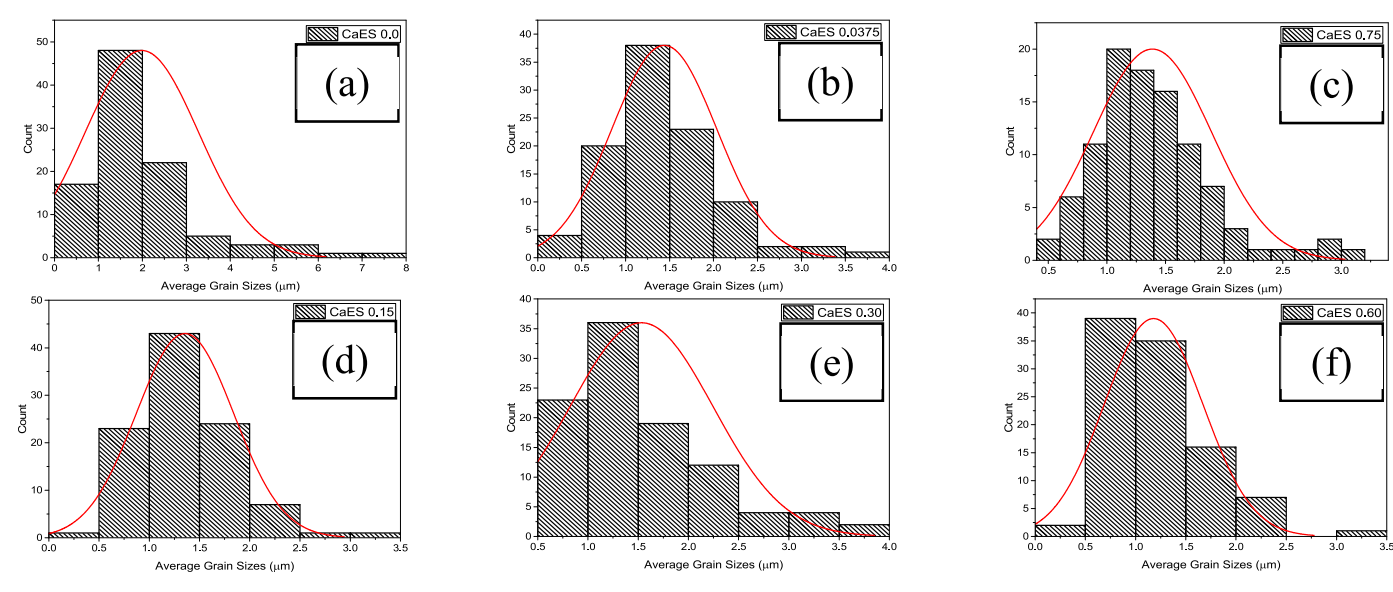


Fig. 5. Grain sizes distribution histograms of YBCO with CaES additions (a)–(f) 0.0000 wt%, 0.0375 wt%, 0.0750 wt%, 0.1500 wt%, 0.3000 wt% and 0.6000 wt% sintered under ambient conditions.

Table 3Average grain sizes for all specimens of YBCO with various concentration of CaES additions sintered under ambient conditions.

CaES Concentrations (wt.%)	0.0000	0.0375	0.0750	0.1500	0.3000	0.6000
Average Grain Sizes (µm)	\sim 1.9887 (\pm 1.2873)	\sim 1.4403 (\pm 0.5967)	\sim 1.3878 (\pm 0.5050)	\sim 1.3555 (\pm 0.4868)	\sim 1.5334 (\pm 0.7133)	~1.1794 (±0.4912)

The atomic % of each element in each specimen was listed in Table 4. From the atomic ratio of all specimens, it is proven that all specimens yield as pure YBCO compound. This is in good agreement with XRD data. For detailing capture the high resolution of EDX mapping analysis on the as-prepared CaES specimen addition of 0.0375 wt%, it proved that Ca element appearance with 0.09 atomic %. This means that the addition of very low concentration i.e., 0.0375 wt% of Ca-compounds appear within grain boundary with improving superconducting properties. Other than that, the existence of C elements in the EDX spectra scanning were attributed from the carbon tape of the sample holder. Hence, it can be neglected.

3.3. Electrical resistivity analysis

The superconducting properties i.e., electrical resistivity measurement of the specimens was measured using the inhouse homemade setup four-point probe technique. The determination of electrical resistivity, ρ against temperature (T) for various CaES addition series (Figs. 7 and 8) and their corresponding derivative are shown in Fig. 9. From Fig. 7, all the CaES addition specimens denoted metallic behavior in the normal state above onset critical transition temperature, $T_{c-onset}$. The values of T_{c-onset} practically were slightly varying with the inclusion of CaES. It is clear that CaES addition affected the normal and superconducting state of samples [54]. This is despite significant changes in the grain boundaries as the inclusions of CaES. Refer to Fig. 8, pure YBCO and specimen with the concentration of 0.0375 wt% and 0.0750 wt% show a single-step transition, however, is changed to double-step transition with higher concentration such as 0.1500 wt%, 0.3000 wt% and 0.6000 wt%. The single step transition was attributed to the highest orthorhombicity (Table 2) and highly composed of Y-123 phase (Table 1) [47]. The samples showed a single-step transition reflecting good grain connectivity and dominance of Y-123 phase [10,55]. The double-step transition implied the presence of other impurity phases CaCuO2 and Ba₄CaCu₃O_{8.61} as analyzed in XRD data and shown in Table 1. Some researchers proposed that double transition was an intrinsic property of highly oxidised Y-123 [56-58]. The higher concentration of impurity

inclusion caused the reduction of the coupling strength among grains.

Table 5 shows all the tabulated critical parameters, and these results were then analyzed and presented in the form of graphs in Figs. 10 and 11 for clearer comparison. Table 5 shows the values of the $T_{\text{c-onset}}$ were not significantly changed with slightly varying of $T_{\rm R}=0$. However, the width of the transition temperatures ΔT_c increased except at the deficient concentrations of CaES, 0.0375 wt% (Fig. 10). The increase of the $\Delta T_{\rm c}$ probably due to the degradation of the local homogeneity within the specimens such as line crack, grains degradation, pores, voids, and many others. This result was good agreement with the EDX and FESEM results. As known, the T_c is a crucial superconducting parameter for the YBCO system, with an increase indicating higher oxygen content. Oxygen content influences YBCO's structure, shifting it from tetragonal (oxygen content \leq 6.5) to orthorhombic (oxygen content \geq 6.5). The superconductivity mechanism is closely linked to Cu-O chains, and disorder in these chains can affect YBCO-123's electrical properties [59,60]. YBCO's T_c remains constant within an oxygen content range of \geq 6.8 to 7.0. Hence, the inclusion of CaES as APCs affects T_c ; for instance, $T_{c-onset}$ is enhanced with 0.0375 wt% CaES due to its impact on normal and superconducting states and significant changes in grain boundaries. This enhances coupling strength among grains, leading to decreased ΔT_c . The lowest concentration of CaES, 0.0375 wt%, with the lowest ΔT_c , indicates good superconducting properties in the specimens.

The transition was made more evident by the plot of $d\rho/dT$ (Fig. 9) which was a result of the resistivity analysis. This plot shows that the mean field transition temperature, $T_{\rm c}^{\rm MF}$ decreased monotonously as listed in Table 5. This peak temperature reflected the superconducting transition within the grains. These findings implied that the inclusion of CaES compound particles caused intragranular alterations. Above the $T_{\rm c}^{\rm MF}$ the conductivity was enhanced by superconducting thermal fluctuation in the normal state [61], whereas the effect of the granularity become dominant in the interval from $T_{\rm c}^{\rm MF}$ down to $T_{\rm c(R=0)}$ [62]. Moreover, the data curves shown a broadening of peaks as shown in Fig. 9 as a result of changed in intergranular properties [63]. However, a tail peak was seen other than the $T_{\rm c}^{\rm MF}$ peak in the high concentration specimens. This might relate to the lower intergranular coupling [62,

S.H. Yap et al. Results in Materials 26 (2025) 100661

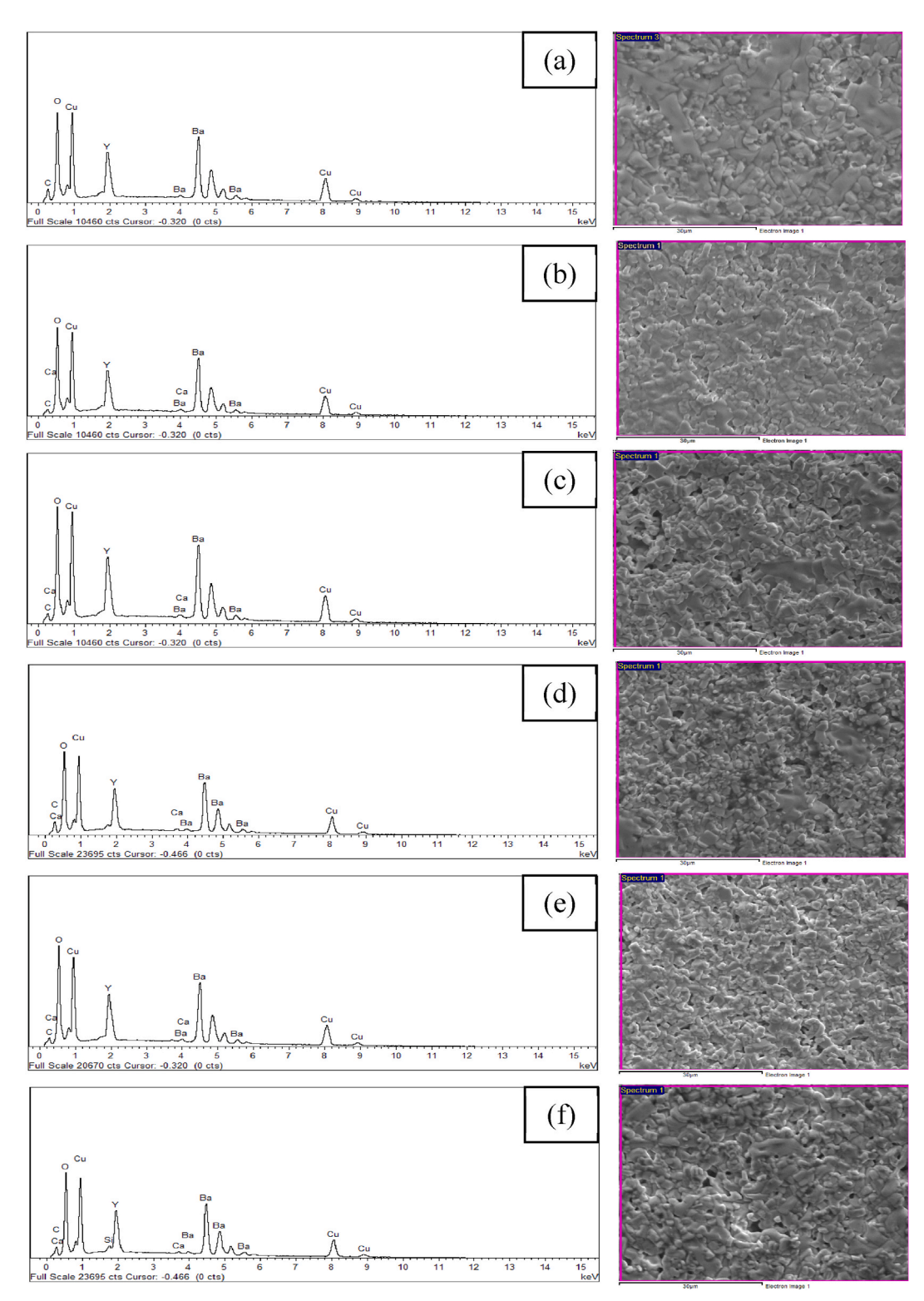


Fig. 6. EDX surface morphology analysis at 10,000x magnification for YBCO with CaES additions (a)–(f): 0.0000 wt%, 0.0375 wt%, 0.0750 wt%, 0.1500 wt%, 0.3000 wt%, and 0.6000 wt% sintered under ambient conditions.

64]. Thus, the intergranular coupling of high concentration specimens (0.15 wt% and above) was weakened as in grain boundary with other phases appearance and oxygen depletion as proof in decreasing orthorhombicity value from the XRD analysis.

Another part of resistivity analysis was identified by the plot of $\rho(T)$ (Fig. 7). It was found that the plots graph was fragmented into two different regions that is non-linear behavior of superconducting regime

and a linear normal state metallic-like behavior which according to the Anderson and Zou relationship [65]:

$$\rho_{\rm n}(T) = \rho_{\rm o} + AT \tag{1}$$

where $\rho_{\rm n}(T)$ is normal state resistivity, A (d ρ /dT) is the calculated slope by linear fitting of resistivity in temperature extend 180 K–250 K and the residual resistivity ρ_0 is extrapolation the linear fitting to 0 K. ρ_0 is the

Table 4The atomic % of elements contained in YBCO with various concentration of CaES additions sintered under ambient conditions.

Specimen (wt.%)	Atomic %						
	Y	Ba	Cu	О	Ca	С	
CaES-0.0000	6.26	14.54	18.64	41.70	-	18.86	
CaES-0.0375	6.94	15.99	22.01	49.13	0.09	5.93	
CaES-0.0750	7.38	15.80	20.88	47.19	0.14	8.60	
CaES-0.1500	6.40	13.02	17.66	43.59	0.44	18.89	
CaES-0.3000	6.74	13.71	18.54	45.46	0.37	15.18	
CaES-0.6000	6.98	15.52	20.06	48.59	0.23	8.62	

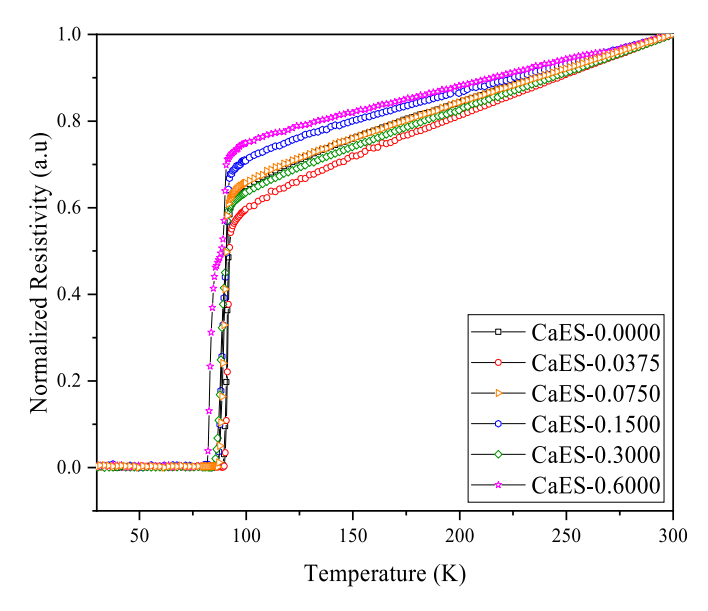


Fig. 7. Normalized resistivity, $(\rho(T))$ analysis for YBCO added with CaES in the various concentrations: 0.0000 wt%, 0.0375 wt%, 0.0750 wt%, 0.1500 wt%, 0.3000 wt% and 0.6000 wt% sintered under ambient conditions.

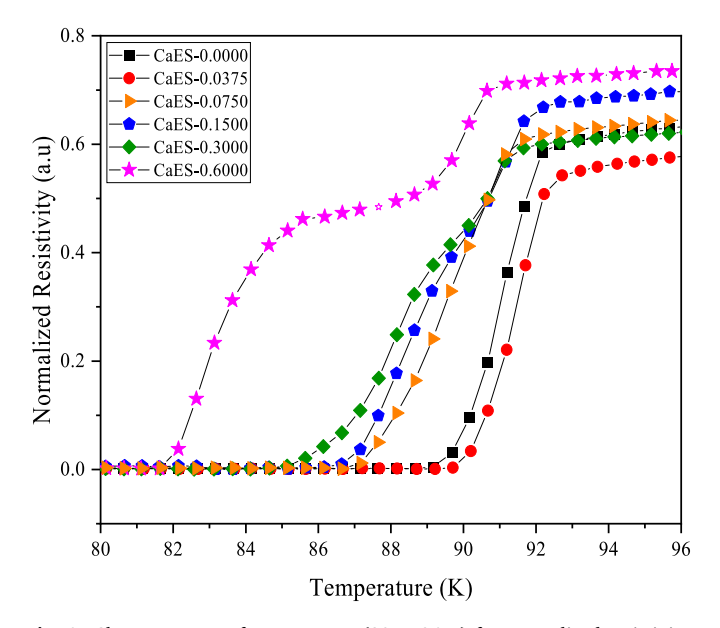


Fig. 8. Close-up range of temperature (80 K–96 K) for normalized resistivity, $(\rho(T))$ analysis for YBCO added with various concentration of CaES sintered under ambient conditions.

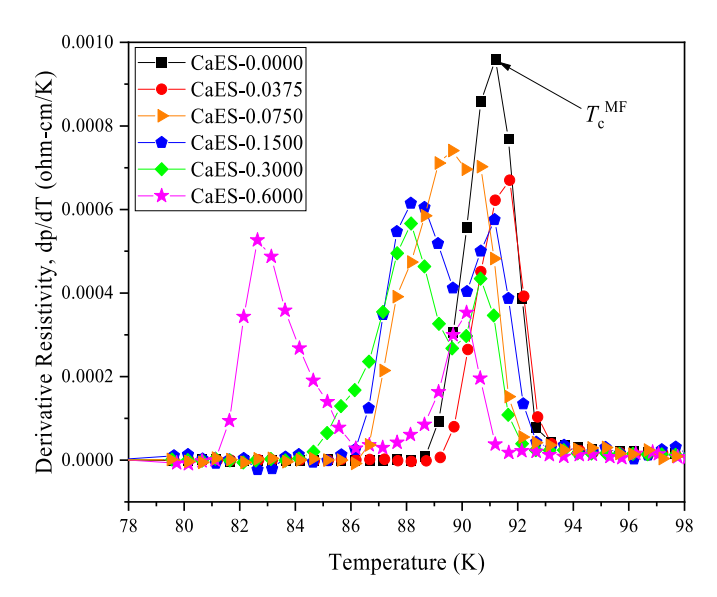


Fig. 9. Derivative resistivity analysis for YBCO added with various concentration of CaES sintered under ambient conditions (close-up range of temperature 78 K–98 K).

residual temperature and its indicator of specimen homogeneity, impurity and defect densities in the specimen. The slope of resistivity, A $(\mathrm{d}\rho/\mathrm{d}T)$ is temperature dependent intrinsic term derives from electron-electron scattering and the diffusion of elementary excitations. The various superconducting parameters can be deduced from the fitting graph, summarized in Table 5 and Figs. 10 and 11. Moreover, the variation of $T_{\rm R}=0$ is due to the varying obtained hole carrier concentration (p) in the CuO₂ planes, per CuO ion [66,67] or number of hole per Cu, which can be deduced from the parabolic relationship as follow [10,68,69]:

$$p = 0.16 - \left[\left(1 - \frac{T_{R=0}}{T_{R=0}^{max}} \right) / 82.6 \right]^{0.5}$$
 (2)

As in Fig. 11, the ρ_0 is decreasing with addition of the lowest concentration, 0.0375 wt% CaES. It is apparent that ρ_0 rises gradually with the increase in the concentration of CaES. This is qualified to the intensification of disorder, inhomogeneities and defects in the specimens [24–26]. Moreover, the rise in ρ_0 implies a lessening in the concentration of charge carriers in the cuprate, which generate a dropping in $T_{\rm R}=_0$. $T_{\rm R}=_0$ is defined as the critical transition temperature at which the $\rho=0$. As shown in Table 5 and Fig. 10, $T_{\rm R}=_0$ varies with the increase in the concentration of CaES. The variations of $T_{\rm R}=_0$ mainly due to the rise of disorder, homogeneities, and characteristics of the addition CaES at grains boundaries [24]. This is in accordance with the FESEM findings.

4. Conclusion

In conclusion, YBCO system enhancements with varying concentrations of CaES were effectively produced using the thermal treatment method under ambient conditions. All specimens showed a good orthorhombic crystal structure with clear intensity of other phases such as BaCuO₂, and Y-211 as shown in XRD analysis. However, there are other non-superconducting phases such as CaCuO₂ and Ba₄CaCu₃O_{8.61} phase had seen in high concentration more than lower concentration addition into the specimen. Surprisingly, the superconducting properties such as $T_{\text{c-onset}}$, $T_{\text{c(R = 0)}}$, ΔT_{c} , ρ_{o} , and p improved after Ca-compounds addition into the YBCO system with the low average grains size for the lowest concentration i.e., 0.0375 wt%. Consequently, it's hole concentration, p reached the highest value (p = 0.16000) among all the specimens with the lowest superconducting transition width, ΔT_{c} =

Table 5The superconducting parameters for YBCO added with various concentration of CaES derived from electrical resistivity measurement.

Specimen (wt.%)	$T_{\text{c-onset}}$ (K)	$T_{c(R=0)}(K)$	$\Delta T_{\rm c}$ (K)	$T_{\rm c}^{\rm MF}$ (K)	Charge Densities $(T_{R=0}/T_{R=0}^{max})$	ρ _o (μohm-cm)	A (μohm-cm/K)	Hole Concentration (<i>p</i>)
CaES-0.0000	93.189	88.868	4.321	91.200	0.9938	1100	3.4314	0.1514
CaES-0.0375	93.223	89.418	3.805	91.711	1.0000	659	2.8936	0.1600
CaES-0.0750	92.172	86.687	5.485	90.670	0.9695	1370	4.1754	0.1408
CaES-0.1500	92.670	86.261	6.409	91.171	0.9647	1540	3.2420	0.1393
CaES-0.3000	92.157	84.823	7.334	90.664	0.9486	1140	3.9184	0.1351
CaES-0.6000	91.678	81.228	10.450	90.160	0.9084	1080	3.1140	0.1267

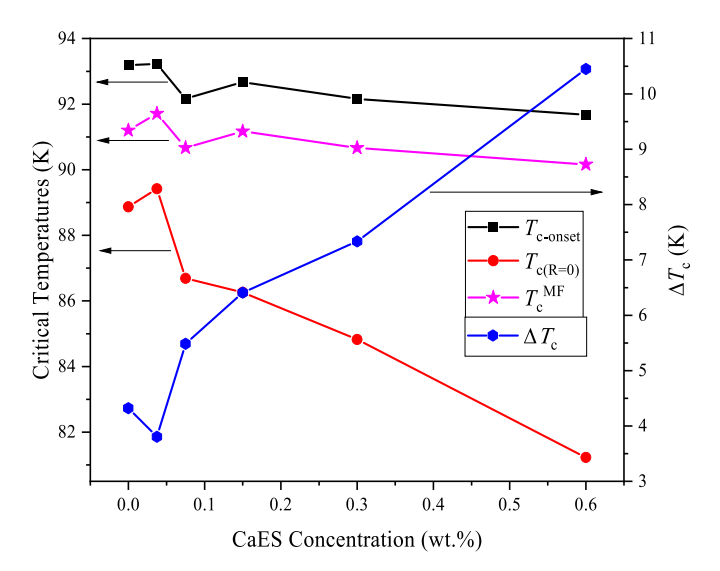


Fig. 10. The comparison of critical temperatures and ΔT_c for YBCO added with various concentration of CaES sintered under ambient conditions.

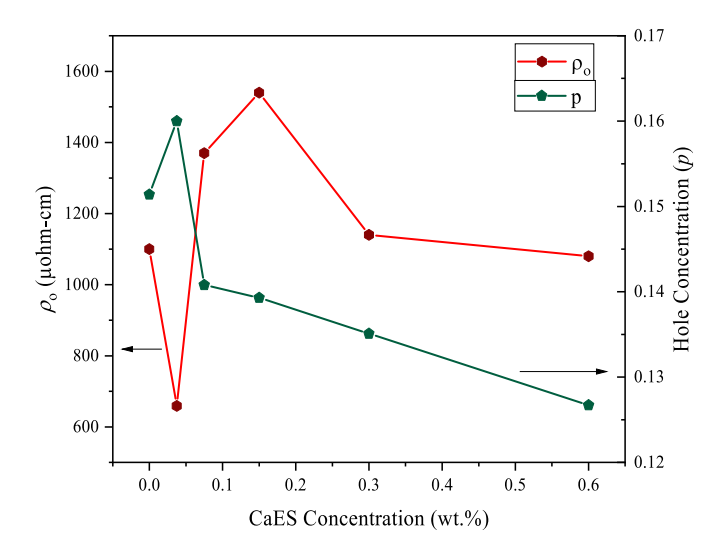


Fig. 11. The comparison of residual resistivity, ρ_0 with the hole concentration, p for YBCO added with various concentration of CaES intered under ambient conditions.

3.805 K ($T_{\text{c-onset}} = 93.223$ K and $T_{\text{c(R} = 0)} = 89.418$ K). The superconducting analysis shows positive results of the lowest residual resistivity, ρ_0 and the highest hole concentration. Hence, the Cacompounds added into YBCO system with the lowest concentration indicated better grain degradation and compactness surface morphology without affecting the average grains size but improving the oxygen ordering in the matrix system. It's exhibited higher p as designated better coupling among the grains with stronger Josephson junction. In

the other points, that may also be due to the homogeneous distribution and sufficient amount of the other phases of ${\rm BaCuO_2}$ and Y-211 that generates and introduced as effective flux pinning site with the strengthening of inter-granular coupling, and it definitely were function as an essential factor to the improvement of p or J_c which will well study in future research. Additionally, this comparison analysis emphasizes the significance of alkali earth metals, particularly when added with a deficient concentration of Ca in the YBCO system synthesized under ambient conditions. This intriguing discovery suggests that further investigations into sintering conditions under the flow of oxygen gas are validated.

CRediT authorship contribution statement

Siew Hong Yap: Writing - review & editing, Writing - original draft, Visualization, Resources, Methodology, Investigation, Formal analysis, Data curation, Conceptualization. Mohd Mustafa Awang Kechik: Writing - review & editing, Visualization, Validation, Supervision, Resources, Project administration, Funding acquisition. Syahrul Humaidi: Funding acquisition, Validation, Supervision. Khairul Khaizi Mohd Shariff: Validation, Supervision. Hussien Baqiah: Validation, Supervision, Conceptualization. Soo Kien Chen: Validation, Supervision. Kean Pah Lim: Validation, Supervision. Mohd Hafiz Mohd Zaid: Validation, Supervision, Resources. Yazid Yaakob: Validation, Supervision, Mohd Khalis Abdul Karim: Validation, Supervision, Zainal Abidin Talib: Validation, Supervision. Zhi Wei Loh: Resources, Methodology. Aliah Nursyahirah Kamarudin: Resources, Methodology, Data curation, Abdul Halim Shaari: Validation, Supervision, Muralidhar Miryala: Writing - review & editing, Funding acquisition, Conceptualization.

Author declarations

The authors declare that they have no known competing financial interest or personal relationships that could have appeared to influence the work reported in this paper.

Declaration of competing interest

The authors declare the following financial interests/personal relationships which may be considered as potential competing interests: Muhd Mustafa Awang Kechik reports financial support, administrative support, article publishing charges, equipment, drugs, or supplies, statistical analysis, travel, and writing assistance were provided by Malaysia Ministry of Higher Education. Muralidhar Miryala reports financial support was provided by Japan Science and Technology Agency. If there are other authors, they declare that they have no known competing financial interests or personal relationships that could have appeared to influence the work reported in this paper.

Acknowledgments

Authors gratefully acknowledge financial support from Ministry of High Education Malaysia (MOHE) for Fundamental Research Grant Scheme FRGS/1/2019/STG02/UPM/02/3 (5540282) Universiti Putra

Malaysia. Syahrul Humaidi would like to thank LP USU under scheme Equity Project: PKUU-PT QS WUR RANK 101-300; LPDP No: 25/UN5.2.3.1/PPM/KPEP/2023 date: 28 December 2023. The paper was partly supported by Japan Science and Technology (JST) for the advanced Project Based Learning (aPBL), Shibaura Institute of Technology (SIT) under the Top Global University Project designed by the Ministry of Education, Culture, Sports, and Science & Technology, Japan.

Data availability

Data will be made available on request.

References

- [1] D.W. Hazelton, V. Selvamanickam, Proc. IEEE 97 (11) (2009) 1831.
- [2] Y. Zhao, J.S. Wang, S.Y. Wang, Z.Y. Ren, H.H. Song, X.R. Wang, C.H. Cheng, Phys. C Supercond. (2004) 412–414, 771.
- [3] D. Larbalestier, A. Gurevich, D.M. Feldmann, A. Polyanskii, Nature 414 (6861) (2001) 368.
- [4] J. Feighan, A. Kursumovic, J. MacManus-Driscoll, Supercond. Sci. Technol. 30 (12) (2017) 123001.
- [5] H. Kaur, H. Kaur, A. Sharma, Mater. Today: Proc. 37 (2021) 3612.
- [6] A.A. Abdul Hussein, A.M. Abdul Hussein, N.A. Hasan, Journal of Applied Sciences and Nanotechnology 3 (1) (2023) 65.
- [7] S. Yawirach, P. Wannasut, P. Boonsong, A. Watcharapasorn, J. Phys.: Conf. Ser. 2431 (1) (2023) 012099.
- [8] E. Hannachi, Y. Slimani, F.B. Azzouz, A. Ekicibil, Ceram. Int. 44 (15) (2018) 18836.
- [9] A.N. Kamarudin, M.M. Awang Kechik, M. Miryala, S. Pinmangkorn, M. Murakami, S.K. Chen, H. Baqiah, A. Ramli, K.P. Lim, A.H. Shaari, Coatings 11 (4) (2021) 377.
- [10] N.M. Hapipi, S.K. Chen, A.H. Shaari, M.M.A. Kechik, K.B. Tan, K.P. Lim, J. Mater. Sci. Mater. Electron. 29 (21) (2018) 18684.
- [11] N.M. Hapipi, S.K. Chen, A.H. Shaari, M.M.A. Kechik, K.B. Tan, K.P. Lim, O.J. Lee, J. Supercond. Nov. Magnetism 32 (5) (2019) 1191.
- [12] M.M. Dihom, A.H. Shaari, H. Baqiah, N.M. Al-Hada, S.K. Chen, M.M.A. Kechik, R. Abd-Shukor, Effects of calcination temperature on microstructure and superconducting properties of Y123 ceramic prepared using thermal treatment method, in: Solid State Phenomena, vol. 268, Trans Tech Publ, 2017, p. 325.
- [13] M.M. Dihom, A.H. Shaari, H. Baqiah, N.M. Al-Hada, C.S. Kien, R.S. Azis, M.M. A. Kechik, Z.A. Talib, R. Abd-Shukor, Results Phys. 7 (2017) 407.
- [14] M.M. Dihom, A.H. Shaari, H. Baqiah, N.M. Al-Hada, Z.A. Talib, C.S. Kien, R.S. Azis, M.M.A. Kechik, L.K. Pah, R. Abd-Shukor, Ceram. Int. 43 (14) (2017) 11339.
- [15] M.M. Awang Kechik, Improvement of Critical Current Density in YBa₂Cu₃O₇₋₈ Films with Nano-Inclusions. University of Birmingham, University of Birmingham, United Kingdom, 2011.
- [16] A. Ramli, N. Manhoril, W.N.W. Mansor, Journal of Sustainability Science and Management 15 (3) (2020) 3.
- [17] M. Murakami, M. Morita, K. Doi, K. Miyamoto, Jpn. J. Appl. Phys. 28 (7R) (1989) 1189.
- [18] T.G. Holesinger, L. Civale, B. Maiorov, D.M. Feldmann, J.Y. Coulter, D.J. Miller, V. A. Maroni, Z. Chen, D.C. Larbalestier, R. Feenstra, X. Li, Y. Huang, T. Kodenkandath, W. Zhang, M.W. Rupich, A.P. Malozemoff, Adv. Mater. 20 (3) (2008) 391.
- [19] L. Calore, M.M. Rahman Khan, S. Cagliero, A. Agostino, M. Truccato, L. Operti, J. Alloys Compd. 551 (2013) 19.
- [20] N.A. Khalid, M.M.A. Kechik, N.A. Baharuddin, C.S. Kien, H. Baqiah, N.N.M. Yusuf, A.H. Shaari, A. Hashim, Z.A. Talib, Ceram. Int. 44 (8) (2018) 9568.
- [21] N.A. Khalid, M.M. Awang Kechik, N.A. Baharuddin, C.S. Kien, H. Baqiah, L.K. Pah, A.H. Shaari, Z.A. Talib, A. Hashim, M. Murakami, J. Mater. Sci. Mater. Electron. 31 (19) (2020) 16983.
- [22] S. Dadras, M. Davoudiniya, S. Dehghani, J. Supercond. Nov. Magnetism 30 (9) (2017) 2451.
- [23] D.-X. Yan, K. Dai, Z.-D. Xiang, Z.-M. Li, X. Ji, W.-Q. Zhang, J. Appl. Polym. Sci. 120 (5) (2011) 3014.
- [24] B. Sahoo, S. Mohapatra, A. Singh, D. Samal, D. Behera, Ceram. Int. 45 (6) (2019) 7709.
- [25] L. Civale, Supercond. Sci. Technol. 10 (7A) (1997) A11.
- [26] S.-L. Huang, M.R. Koblischka, K. Fossheim, T.W. Ebbesen, T.H. Johansen, Phys. C Supercond. 311 (3) (1999) 172.
- [27] P.S. Mukherjee, A. Simon, M.S. Sarma, A.D. Damodaran, Solid State Commun. 81 (3) (1992) 253.
- [28] I. Nedkov, A. Veneva, J. Appl. Phys. 75 (10) (1994) 6726.

- [29] M.M. Dihom, A.H. Shaari, H. Baqiah, C.S. Kien, R.S. Azis, R. Abd-Shukor, N.M. Al-Hada, M.M.A. Kechik, Z.A. Talib, J. Supercond. Nov. Magnetism 32 (7) (2019) 1875.
- [30] K. Matsumoto, P. Mele, Supercond. Sci. Technol. 23 (1) (2009) 014001.
- [31] K. Matsumoto, T. Horide, K. Osamura, M. Mukaida, Y. Yoshida, A. Ichinose, S. Horii, Phys. C Supercond. (2004) 412–414, 1267.
- [32] P. Mikheenko, J. Abell, A. Sarkar, V. Dang, M.A. Kechik, J. Tanner, P. Paturi, H. Huhtinen, N.H. Babu, D. Cardwell, J. Phys.: Conf. Ser. 234 (2) (2010) 022022.
- [33] N.A. Khalid, W. Kong, I. Kong, C. Kong, M.M.A. Kechik, R. Abd-Shukor, Nano Hybrids and Composites, vol. 31, 2021, p. 1.
- [34] Y. Jiang, S. Decker, C. Mohs, K.J. Klabunde, J. Catal. 180 (1) (1998) 24.
- [35] M. Frietsch, F. Zudock, J. Goschnick, M. Bruns, Sensor. Actuator. B Chem. 65 (1) (2000) 379.
- [36] R. Al-Gaashani, S. Radiman, N. Tabet, A.R. Daud, Mater. Chem. Phys. 125 (3) (2011) 846.
- [37] E. Comini, C. Baratto, G. Faglia, M. Ferroni, A. Vomiero, G. Sberveglieri, Prog. Mater. Sci. 54 (1) (2009) 1.
- [38] G. Malandrino, A. Frassica, G.G. Condorelli, G. Lanza, I.L. Fragalà, J. Alloys Compd. 251 (1) (1997) 314.
- [39] T. Jarlborg, Phys. C Supercond. 454 (1) (2007) 5.
- [40] F. Suzuki, P.-Y. Wang, J. Weatherspoon, L. Mead, in: D.P.A. Publication (Ed.), Method of Producing Eggshell Powder, 2004.
- [41] R. Mohadi, K. Anggraini, F. Riyanti, A. Lesbani, Sriwijaya Journal of Environment 1 (2) (2016) 32.
- [42] N.N. Mohd Yusuf, M.M. Awang Kechik, H. Baqiah, C. Soo Kien, L. Kean Pah, A. H. Shaari, W.N.W. Wan Jusoh, A. Sukor, S. Izzati, M. Mousa Dihom, Mater 12 (1) (2019) 92.
- [43] M.G. Naseri, E.B. Saion, M. Hashim, A.H. Shaari, H.A. Ahangar, Solid State Commun. 151 (14) (2011) 1031.
- [44] M. Goodarz Naseri, E.B. Saion, H. Abbastabar Ahangar, A.H. Shaari, M. Hashim, J. Nanomater. (2010) 907686, 2010.
- [45] N.A.M. Yamin, M.H.M. Zaid, K.A. Matori, J.L.Y. Chyi, S.N.F. Zalamin, N.A. N. Ismail, K.F. Chan, N. Effendy, Appl. Phys. A 128 (1) (2022) 93.
- [46] A. Bhargava, I.D.R. Mackinnon, T. Yamashita, D. Page, Phys. C Supercond. 241 (1) (1995) 53.
- [47] A. Ramli, A.H. Shaari, H. Baqiah, C.S. Kean, M.M.A. Kechik, Z.A. Talib, J. Rare Earths 34 (9) (2016) 895.
- [48] A. Bahboh, A.H. Shaari, H. Baqiah, C.S. Kien, M.M.A. Kechik, M.H. Wahid, R. Abd-Shukor, Z.A. Talib, Ceram. Int. 45 (11) (2019) 13732.
- [49] E. Nazarova, A. Zaleski, A. Zahariev, A. Stoyanova-Ivanova, K. Zalamova, Phys. C Supercond. 403 (4) (2004) 283.
- [50] A.H. Salama, M. El-Hofy, Y.S. Rammah, M. Elkhatib, Adv. Nat. Sci. Nanosci. Nanotechnol. 6 (4) (2015) 045013.
- [51] A. Ono, Jpn. J. Appl. Phys. 26 (Part 2, No. 7) (1987) L1223.
- [52] P. Benzi, E. Bottizzo, N. Rizzi, J. Cryst. Growth 269 (2) (2004) 625.
- [53] K. Nagashio, Y. Takamura, K. Kuribayashi, Y. Shiohara, J. Cryst. Growth 200 (1) (1999) 118.
- [54] E. Hannachi, Y. Slimani, A. Ekicibil, A. Manikandan, F.B. Azzouz, Mater. Chem. Phys. 235 (2019) 121721.
- [55] I. Hamadneh, A.M. Rosli, R. Abd-Shukor, N.R.M. Suib, S.Y. Yahya, J. Phys.: Conf. Ser. 97 (2008) 012063.
- [56] H. Claus, U. Gebhard, G. Linker, K. Röhberg, S. Riedling, J. Franz, T. Ishida, A. Erb, G. Müller-Vogt, H. Wühl, Phys. C Supercond. 200 (3–4) (1992) 271.
- [57] D. Dimos, P. Chaudhari, J. Mannhart, Phys. Rev. B 41 (7) (1990) 4038.
- [58] E. Janod, A. Junod, T. Graf, K.Q. Wang, G. Triscone, J. Muller, Phys. C Supercond. 216 (1) (1993) 129.
- [59] J. Jorgensen, M.A. Beno, D.G. Hinks, L. Soderholm, K. Volin, R. Hitterman,
- J. Grace, I.K. Schuller, C. Segre, K. Zhang, Phys. Rev. B 36 (7) (1987) 3608.
- [60] Y. Suyama, M. Matsumoto, S. Kageyama, I. Sato, Effect of oxygen deficiency on the superconducting properties of YBCO, in: Presented at Advances in Superconductivity, vol. III, 1991. Tokyo.
- [61] P. Pureur, R.M. Costa, P. Rodrigues Jr, J. Schaf, J.V. Kunzler, Phys. Rev. B 47 (17) (1993) 11420.
- [62] A.R. Jurelo, I.A. Castillo, J. Roa-Rojas, L.M. Ferreira, L. Ghivelder, P. Pureur, P. Rodrigues, Phys. C Supercond. 311 (1) (1999) 133.
- [63] A. Mohanta, D. Behera, Phys. C Supercond. 470 (4) (2010) 295.
- [64] H. Salamati, P. Kameli, Solid State Commun. 125 (7) (2003) 407.
- [65] Y. Slimani, E. Hannachi, M.K. Ben Salem, A. Hamrita, M.B. Salem, F.B. Azzouz, J. Supercond. Nov. Magnetism 28 (10) (2015) 3001.
- [66] A. Sedky, B. Abu-Ziad, Phys. C (Amsterdam, Neth.): Supercond. Appl. 470 (17) (2010) 659.
- [67] A. Sedky, J. Phys. Chem. Solid. 70 (2) (2009) 483.
- [68] A. Mellekh, M. Zouaoui, F.B. Azzouz, M. Annabi, M.B. Salem, Solid State Commun. 140 (6) (2006) 318.
- [69] M.A. Almessiere, E. Hannachi, Y. Slimani, G. Yasin, M. Mumtaz, M.R. Koblischka, A. Koblischka-Veneva, A. Manikandan, A. Baykal, Mater. Chem. Phys. 243 (2020) 122665.